Thermal wind analysis using single-Doppler radar data

R.Hannesen and A.Weipert, Selex-Gematronik, Neuss, Germany

1. Algorithm Description

Vertical profiles of the 3D wind vector and linear derivatives of the wind field can be derived from single Doppler radar data using the Volume Velocity Processing (VVP) algorithm according to Waldteufel and Corbin (1979). The algorithm performs least-squares fits of radial velocities measured in three-dimensional areas (volumes).
Among the resulting parameters, the horizontal (2D) or 3D wind vector are the most commonly used. The horizontal derivatives can also be used to calculate the divergence. Additionally, the vertical derivatives can be used to derive the so-called Thermal Wind.
The results allow a detailed analysis of the thermodynamic situation.

The Thermal Wind (more precise: the vertical shear of the horizontal geostrophic Wind $\mathbf{v}_g$) is defined as (Holton 1992, equation 3.30):

$$\frac{\partial \mathbf{v_g}}{\partial \ln p} = -\frac{R}{f} \cdot \mathbf{k} \times \nabla_p T \qquad (1)$$

with p being the pressure, T is the Temperature (in Kelvin), f is the Coriolis parameter, R is the specific Gas Constant, $\mathbf{k}$ is the vertically pointing unit vector, and $\nabla_p = \mathbf{i}\partial/\partial x + \mathbf{j}\partial/\partial y$ is the horizontal Nabla operator (for surfaces of constant pressure).

Equation (1) can be re-arranged using the following relations (with ρ being the air density, and g being the gravity acceleration):

$$p = \rho \cdot R \cdot T \qquad (2a)$$

$$\frac{\partial}{\partial \ln p} = p \cdot \frac{\partial}{\partial p} = \frac{p}{\partial p/\partial z} \cdot \frac{\partial}{\partial z} \qquad (2b)$$

$$\frac{\partial p}{\partial z} = -\rho \cdot g \qquad (2c)$$

$$\Rightarrow \quad \frac{\partial}{\partial \ln p} = -\frac{p}{\rho \cdot g} \cdot \frac{\partial}{\partial z} = -\frac{R \cdot T}{g} \cdot \frac{\partial}{\partial z} \qquad (2d)$$

Henceforth, we omit the g index for $\mathbf{v}$. With the above, equation (1) then reads:

$$-\frac{R \cdot T}{g} \cdot \frac{\partial \mathbf{v}}{\partial z} = -\frac{R}{f} \cdot \mathbf{k} \times \nabla T \qquad (3a)$$

which can be simplified to

$$-\frac{T \cdot f}{g} \cdot \frac{\partial \mathbf{v}}{\partial z} = -\mathbf{k} \times \nabla T \qquad (3b)$$

Multiplying (3b) with $\mathbf{k}\times\mathbf{v}$ and considering that for any vector $\mathbf{a}$ the relation $(\mathbf{k}\times\mathbf{v})\cdot(\mathbf{k}\times\mathbf{a}) = \mathbf{v}\cdot\mathbf{a}$, we get the Temperature Advection A_T (in terms of temperature change per time interval):

$$A_T \equiv -\mathbf{v} \cdot \nabla T = -\frac{T \cdot f}{g} \cdot \frac{\partial \mathbf{v}}{\partial z} \cdot (\mathbf{k} \times \mathbf{v}) \qquad (4a)$$

$$A_T = -\frac{T \cdot f}{g} \cdot \left(u \cdot \frac{\partial v}{\partial z} - v \cdot \frac{\partial u}{\partial z} \right) \qquad (4b)$$

Equation (4b) contains known parameters:

- The horizontal wind components u and v and their vertical derivatives are resulting from the VVP algorithm.
- The Coriolis parameter f can be calculated from the Radar latitude.
- The gravity acceleration g is known.
- The temperature T can be estimated from the known height z using the US Standard Atmosphere.

The last assumption (about the temperature) is valid for most situations with an error of less than ten per cent. This error is less than or comparable to typical errors resulting in the VVP algorithm itself.

The VVP algorithm can be used in a simpler form where only the 3D wind vector $\mathbf{v}$ only or additionally the horizontal derivatives are calculated. In this case the vertical derivatives in (4b) are replaced by the differences between the VVP layer heights:

$$A_T = -\frac{T \cdot f}{g} \cdot \left(u_0 \cdot \frac{\Delta v_0}{\Delta z} - v_0 \cdot \frac{\Delta u_0}{\Delta z} \right) \qquad (5)$$

All the above must be regarded with some precaution:
The derivations are valid for geostrophic wind only (i.e. free of friction forces). In the atmospheric boundary layer of about the lowest kilometer however, frictional forces usually cause some wind shear known as the Ekman spiral (cf. Holton, 1992, chapter 5). In such cases, equation (4b) would lead to a non-zero Temperature Advection even in an isotherm atmosphere.
Also, a significant sea-breeze circulation which can often be found at coastal radar sites does not belong to a geostrophic wind situation. In such cases, the real Temperature Advection is different than calculated from the above equation.
Finally, in tropical regimes the Coriolis parameter f is too small, i.e. turbulent frictional forces are usually larger than Coriolis forces. In such areas, the above assumptions are often not valid and the Temperature Advection is different than calculated from the above equation.

Thermal wind analysis using single-Doppler radar data

R.Hannesen and A.Weipert, Selex-Gematronik, Neuss, Germany

2. Quality Control

The VVP least-squares fit can be performed already with very few independent measurements of the radial velocity within a layer. However, if very few measurements are available only or if the measurements do only cover a small horizontal range (and thus are not independent enough), the result will be affected strongly by outlying measurements causing unrealistic results.

Thus some data Quality Control checks have to be performed before the regression is done. The following quality control steps are included in the Rainbow®5 package (www.gematronik.com):

- **Removal of ground clutter**
  Data with a velocity close to zero (i.e. below a configurable *Minimum Velocity*) are discarded as they may be contaminated by clutter. Also, the *minimum elevation* slice can be selected to remove low-level data which tend to be influenced by ground returns.

- **Sufficient amount of data and horizontal distribution**
  The horizontal area within the minimum and maximum range is subdivided into eight 45-degree sectors. A sector may contain no data but then both neighboring sectors must have at least a configurable *amount of data*.

- **Second regression and elimination of outlying data**
  The VVP algorithm can be performed twice on the measured data. In that case the radial velocity V_r' can be calculated from the VVP results of the first regression for each measurement position and compared with the measured V_r. If the difference between V_r and V_r' is larger than a configurable *Maximum Velocity Difference*, the corresponding measurement V_r is discarded for the second algorithm regression.

- Furthermore, the **standard deviation** is calculated for each layer. If a layer's standard deviation is larger than a configurable *Maximum Standard Deviation*, the corresponding result is flagged to be "not ok".

- If for the second regression too many data have been removed due to the *Maximum Velocity Difference* threshold, it is likely that the results are not reliable at all. This might be the case in very convective situations, where the wind differs significantly from a linear field. Also, if the velocity data are heavily biased, the *Maximum Velocity Difference* threshold usually causes rejection of a large amount of data. For that reason, if more data were removed than a configurable *Maximum Remove Percentage*, the corresponding result is flagged to be "not ok".

The Rainbow®5 Quality Control is essential to obtain reliable results. Holleman (2005) found that with this control being applied, the VVP wind profile data satisfy the WMO requirements for upper-air wind measurements.

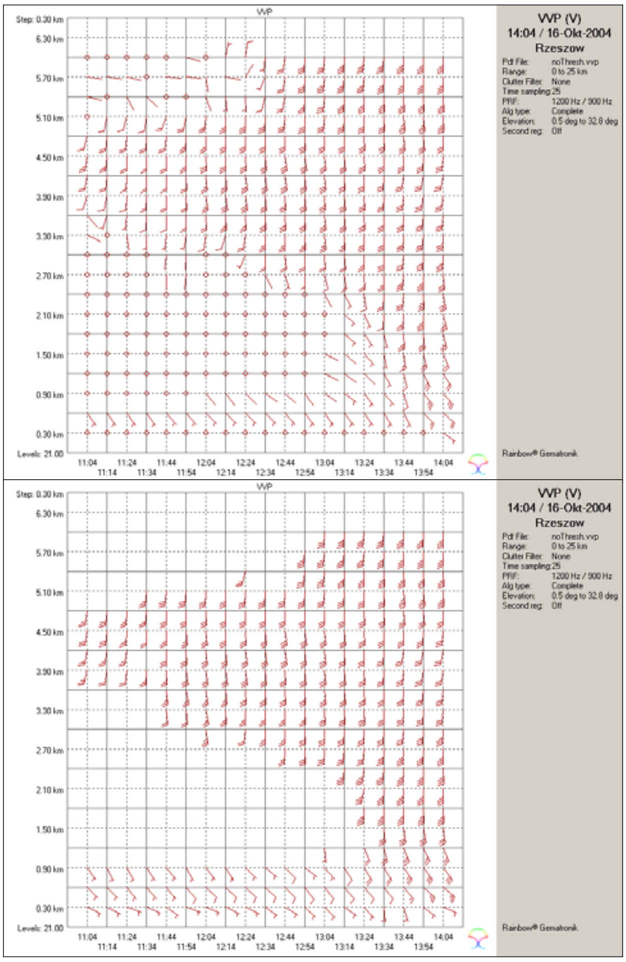

Figure 1: Effects of the Rainbow®5 Quality Control on the VVP algorithm results. Top: without Quality Control, several results have wrong wind speed or direction. Bottom: with Quality Control, the outliers are corrected or flagged out. Data © courtesy of IMGW Poland.

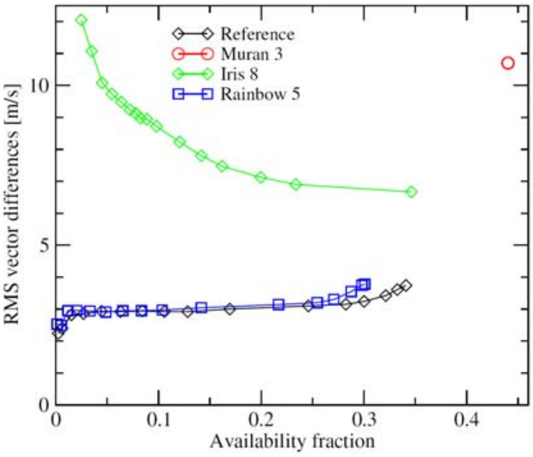

Figure 2: The RMS vector differences between VVP and Hirlam wind vectors as a function of the availability fraction of the VVP wind vectors (the availability fraction is varied by changing the standard deviation threshold, if available). Due to Quality Control, Rainbow®5 provides much better results than other VVP implementations. Image © by KNMI; from Holleman and Beekhuis (2005).

Thermal wind analysis using single-Doppler radar data

R.Hannesen and A.Weipert, Selex-Gematronik, Neuss, Germany

3. Case Study: Cold Front, Rzeszow, Poland, 16-Oct-2004

On 16-Oct-2004, Poland was influenced by a southerly flow. A low-tropospheric trough extended from southern Denmark towards South Poland. Embedded in this trough was a weak cold front which crossed Poland from Southwest towards Northeast. The front crossed the Rzeszow radar site in the late evening of that day.

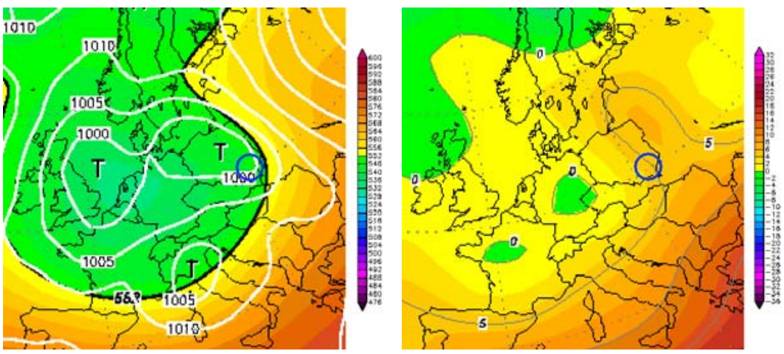

Figure 3: NCEP reanalysis of 17-Oct-2004, 00:00 UTC. Left: sea-level pressure (hPa) and 500hPa height (gpdm, colored). Right: 850 hPa temperature (deg C). The blue circle shows the 125km-range of the Rzeszow radar. Images © from www.wetterzentrale.de

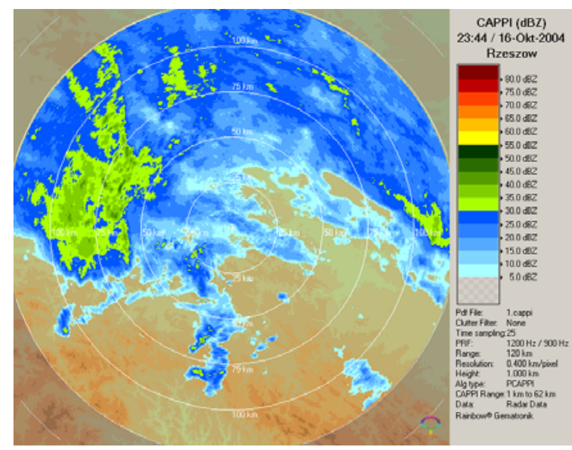

Figure 4: CAPPI Reflectivity from the Rzeszow radar from 16-Oct-2004, 23:44 UTC. Data © courtesy of IMGW Poland.

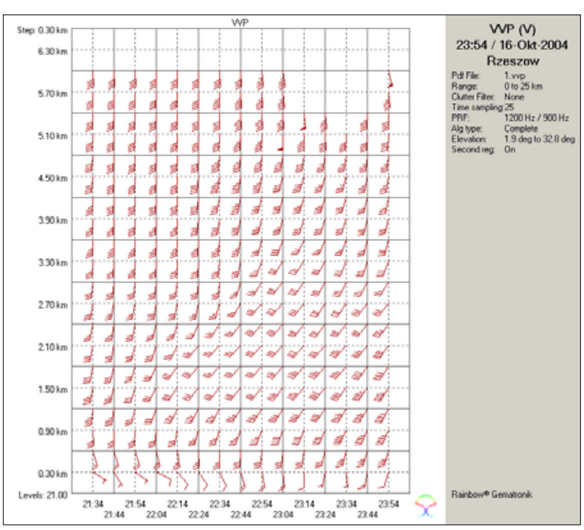

Figure 5: Time series of VVP wind data (vertical profile of horizontal wind). The passage of the cold front is indicated by a change of the wind direction from S to SW, which appears later with increasing time. Data © courtesy of IMGW Poland.

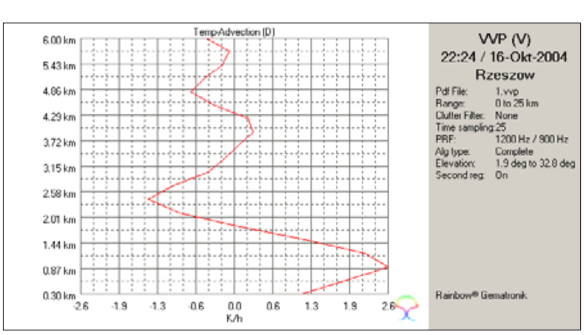

Figure 6: Temperature Advection example obtained from the VVP algorithm. At that time (22:44 UTC), the cold front is strongest at a height of 2.5 km with an cold-air advection of –1.5 K/h. Data © courtesy of IMGW Poland.

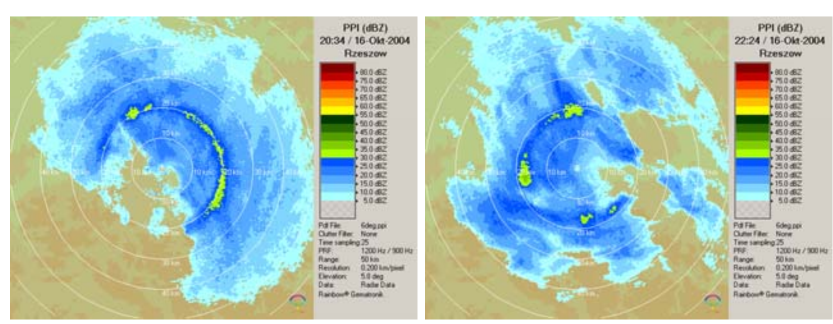

Figure 7: In a 5.8deg-PPI, the bright band appears as a ring and indicates the drop of the melting layer due to the front from about 2.1 km (left) to about 1.8 km (right), corresponding to a temperature drop of about 2 K. Data © courtesy of IMGW Poland.

	21:34	21:44	21:54	22:04	22:14	22:24	22:34	22:44	22:54	23:04	23:14	23:24	23:34	23:44
6.0	-0.3	-0.4	-0.6	-0.7	-0.3	-0.5	-0.3	-0.8	-0.7	-0.5				
5.7	-0.5	-0.4	-0.4	-0.4	-0.2	-0.1	-0.5	-0.3	-0.7	-1.0				
5.4	-0.5	-0.3	-0.2	-0.1	0.0	-0.2	-0.5	-0.6	-0.8	-1.2	-1.3	-3.7		-1.1
5.1	-0.3	-0.2	0.0	0.0	0.0	-0.5	-0.8	-1.0	-1.1	-1.9	-1.9	-1.8	-1.1	-0.4
4.8	-0.1	-0.1	0.0	0.1	-0.1	-0.7	-0.8	-1.2	-1.4	-1.9	-2.2	-1.9	-1.2	-0.8
4.5	0.2	0.0	-0.1	0.0	-0.1	-0.4	-0.5	-0.9	-1.3	-0.8	-1.2	-0.9	-0.8	-0.6
4.2	0.3	0.1	0.0	0.0	0.0	0.2	0.1	-0.2	-0.5	-0.1	0.0	-0.1	-0.2	-0.2
3.9	0.1	0.2	0.1	0.0	0.1	0.3	0.4	0.2	0.0	-0.4	-0.5	-0.4	-0.1	0.0
3.6	-0.1	-0.1	-0.1	-0.1	-0.1	0.1	0.2	0.0	-0.5	-1.2	-1.0	-0.7	-0.3	-0.3
3.3	-0.3	-0.4	-0.3	-0.4	-0.4	-0.2	0.0	-0.4	-1.1	-1.2	-0.7	-0.4	-0.5	-0.9
3.0	-0.4	-0.4	-0.4	-0.4	-0.4	-0.4	-0.6	-1.0	-1.0	-0.6	-0.3	-0.3	-0.8	-1.2
2.7	-0.3	-0.2	-0.3	-0.4	-0.6	-1.0	-1.5	-1.3	-0.6	-0.2	-0.2	-0.6	-0.9	-0.8
2.4	-0.1	0.0	-0.2	-0.5	-1.0	-1.4	-1.4	-0.8	-0.3	-0.1	-0.2	-0.6	-0.6	0.0
2.1	-0.2	-0.2	-0.3	-0.8	-1.1	-0.9	-0.5	-0.2	0.0	0.1	-0.2	-0.4	-0.1	0.3
1.8	-0.2	-0.3	-0.4	-0.7	-0.5	0.1	0.3	0.3	0.3	0.4	-0.1	0.1	0.5	0.6
1.5	0.5	0.3	0.2	0.3	0.8	1.2	1.2	1.0	0.9	1.0	0.9	1.0	1.1	1.0
1.2	1.5	1.3	1.3	1.8	2.1	2.2	2.1	2.0	2.0	2.0	2.5	2.4	2.0	1.8
0.9	1.3	1.4	1.9	2.5	2.7	2.6	2.4	2.5	2.6	2.6	2.9	2.7	2.4	2.0
0.6	0.7	0.6	1.3	2.2	2.0	1.9	1.8	1.8	1.8	1.7	1.5	1.2	1.5	1.1
0.3	0.0	-0.4	0.1	1.3	1.2	1.1	1.2	1.1	0.9	0.4	0.1	-0.1	0.8	0.3

Figure 8: Time series of the vertical profile of Temperature Advection (K/h) obtained from the VVP algorithm. The increasing height of the cold front can be obtained from the layer of cold air advection indicated by the green ellipse. The positive Temperature Advection values below 1.8 km are biased due to boundary layer effects (Ekman spiral). Data © courtesy of IMGW Poland.

Thermal wind analysis using single-Doppler radar data

R.Hannesen and A.Weipert, Selex-Gematronik, Neuss, Germany

4. Case Study: Freezing Rain and Snow, Karlsruhe, Germany, 23-Dec-1996

On 23-Dec-1996, freezing rain occurred across Southwest Germany. The event was caused by a warm and humid southwesterly flow in mid-tropospheric levels and a cold easterly flow in about the lowest kilometer. Thus snow melted at an altitude of 1.5 km and froze on the ground. Later during that day, the cold low-level flow gained vertical extent, and snow could fall down to ground.

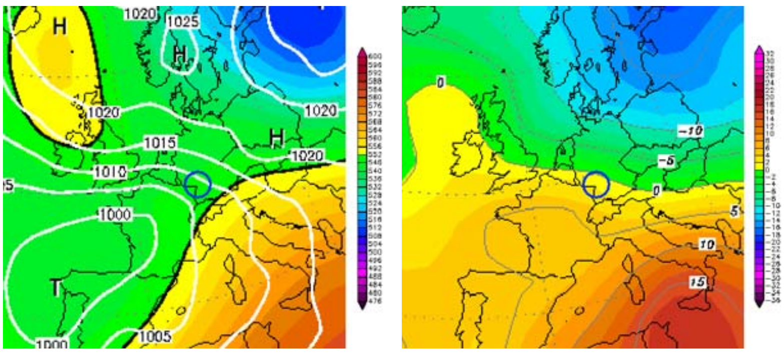

Figure 9: NCEP reanalysis of 23-Dec-1996, 01:00 UTC. Left: sea-level pressure (hPa) and 500hPa height (gpdm, colored). Right: 850 hPa temperature (deg C). The blue circle shows the 120km-range of the Karlsruhe radar. Images © from www.wetterzentrale.de

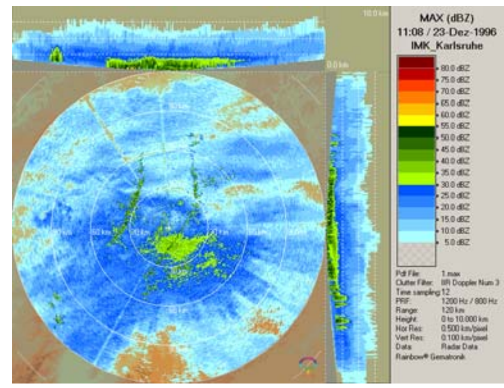

Figure 10: MAX Reflectivity from the Karlsruhe radar from 23-Dec-1996, 11:08 CET (i.e. 10:08 UTC). Data © courtesy of Radar-Info, Karlsruhe, Germany.

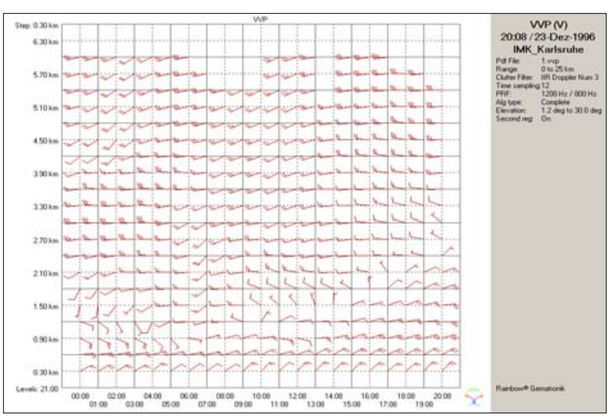

Figure 11: Time series (CET) of VVP wind data (vertical profile of horizontal wind). Above about 1 km, a SW flow brings warm humid air. Below that, a cold E flow dominates causing freezing rain. After noon, the cold low-level flow gained vertical extent, reaching about 2.5 km in the evening. Snow fell down to ground then. Data © courtesy of Radar-Info, Karlsruhe, Germany.

6.0	0.5	0.3	0.6	0.1	0.0	-0.5	0.1					-0.1	0.7	0.7		-0.7	-0.6	-0.6			
5.7	0.2	0.3	0.4	0.0	0.0	-0.2	0.1	0.7				0.2	0.3	0.4		0.0	-0.2	-0.2	0.6	-0.3	
5.4	-0.1	0.3	0.1	0.0	-0.1	0.1	0.1	0.0	0.5	-0.1	-0.3	0.2	0.1	0.0		0.1	0.0	0.0	-0.1	-0.3	0.4
5.1	0.0	0.1	0.3	0.2	-0.1	0.2	0.0	0.0	0.3	0.0	-0.3	-0.1	-0.1	0.0	-0.5	-0.2	-0.1	-0.1	-0.3	-0.3	0.1
4.8	0.5	0.3	0.6	0.1	-0.1	-0.1	-0.1	0.2	0.1	-0.1	-0.2	0.0	-0.1	0.1	-0.2	-0.4	-0.3	-0.4	-0.4	-0.2	0.0
4.5	0.5	0.2	0.1	-0.5	-0.5	-0.4	-0.3	0.1	0.2	-0.1	0.0	0.1	0.0	0.0	0.1	-0.3	-0.5	-0.4	-0.1	-0.1	0.2
4.2	-0.1	-0.4	-0.8	-0.8	-0.7	-0.7	-0.6	-0.3	0.1	-0.2	0.0	0.1	-0.1	0.0	0.1	0.0	-0.1	-0.1	0.1	0.0	0.2
3.9	-0.4	-0.6	-0.8	-0.4	-0.4	-0.4	-0.2	-0.3	-0.1	-0.2	0.0	-0.2	-0.2	-0.2	-0.1	0.2	0.2	0.1	0.0	-0.1	-0.1
3.6	-0.2	0.0	0.0	-0.1	-0.1	0.7	0.8	0.4	-0.1	0.0	-0.1	-0.2	0.0	0.0	-0.1	0.0	0.0	-0.1	-0.1	-0.2	-0.2
3.3	-0.1	0.5	0.4	-0.3	0.2	0.6	0.9	0.7	-0.1	-0.1	-0.3	0.1	0.2	0.2	0.3	0.0	-0.1	-0.1	0.0	-0.1	-0.2
3.0	0.1	0.3	0.3	-0.4	0.2	-0.3	0.2	0.6	0.1	-0.3	-0.4	-0.2	-0.1	0.0	0.1	0.1	0.1	0.1	0.1	0.0	-0.1
2.7	0.3	0.5	0.2	-0.2	0.0	-0.4	-0.4	0.5	0.3	-0.1	-0.3	-0.7	-0.4	-0.1	-0.1	0.0	0.1	0.1	0.1	0.0	-0.1
2.4	0.5	0.9	0.4	0.1	0.0	-0.2	-0.5	0.0	-0.1	0.0	-0.2	-0.7	-0.5	-0.3	-0.1	0.0	-0.1	-0.1	-0.1	-0.1	-0.2
2.1	0.7	0.7	0.4	0.2	0.2	0.0	-0.3	-0.2	-0.3	-0.2	-0.3	-0.4	-0.5	-0.5	-0.4	-0.2	-0.2	-0.2	-0.1	0.0	-0.1
1.8	0.3	0.4	0.3	0.3	0.3	0.1	-0.2	-0.1	-0.1	-0.1	-0.3	-0.2	-0.3	-0.4	-0.4	-0.3	-0.2	-0.3	-0.2	-0.3	-0.4
1.5	0.3	0.5	0.4	0.3	0.5	0.4	0.1	-0.2	0.0	-0.1	-0.4	-0.3	-0.3	-0.3	-0.2	-0.1	-0.1	-0.2	-0.4	-0.5	-0.6
1.2	0.1	0.4	0.6	0.5	0.9	0.5	0.2	-0.1	0.0	-0.2	-0.6	-0.6	-0.3	-0.1	0.0	0.0	0.1	-0.1	0.1	0.3	0.7
0.9	0.9	1.3	1.5	1.5	1.4	0.5	0.2	0.0	0.0	0.0	0.0	0.1	0.4	0.5	0.7	0.6	0.8	0.8	1.1	1.3	1.6
0.6	1.7	1.9	2.0	1.6	1.3	0.5	0.4	0.3	0.4	0.5	0.7	0.9	1.0	0.9	0.9	1.0	1.1	1.2	1.2	1.2	1.3
0.3	0.7	0.8	1.0	0.4	0.6	0.2	0.4	0.4	0.4	0.7	0.5	0.6	0.7	0.5	0.5	0.7	0.6	0.7	0.6	0.6	0.6
	0:08	1:08	2:08	3:08	4:08	5:08	6:08	7:08	8:08	9:08	10:08	11:08	12:08	13:08	14:08	15:08	16:08	17:08	18:08	19:08	20:08

Figure 12: Time series (CET) of the vertical profile of Temperature Advection (K/h) obtained from the VVP algorithm. Between 1 and 3 km altitude and before noon, warm air was advected (left green ellipse); causing freezing rain. Later, cold air advection lasting for several hours (right ellipse) resulted in snowfall to the ground. Advection values below 1.2 km are biased due to boundary layer effects (Ekman spiral). Data © courtesy of Radar-Info, Karlsruhe.

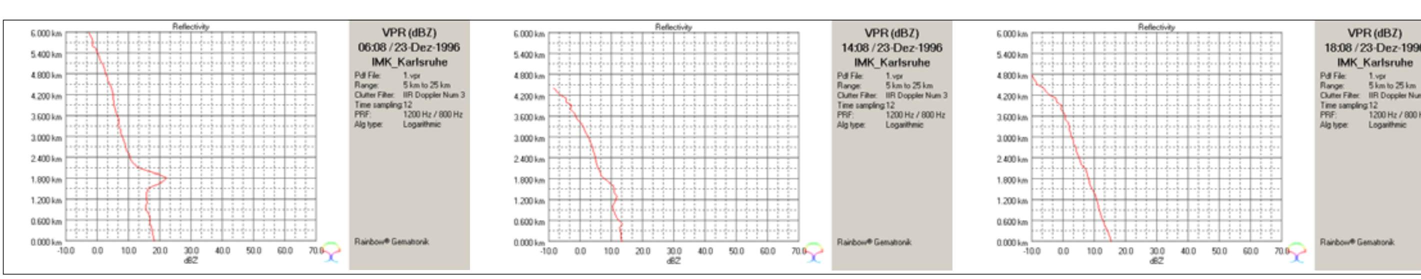

Figure 13: Vertical profiles of Reflectivity (VPR). Left: at 06:08 CET, a well established bright band peaks at 1.8 km altitude. Center: at 14:08 CET, the bright band has lowered to 1.3 km and became very weak. Right: at 18:08 CET, the bright band has gone. Data © courtesy of Radar-Info, Karlsruhe.

Acknowledgements

The authors are grateful to R. Lewandowski from IMGW, Poland, for providing the Rzeszow C-Band Doppler Radar data, and to H. Gysi from Radar-Info, Karlsruhe, Germany, for providing the Karlsruhe C-Band Doppler Radar data.

References

Holleman, I. (2005): *Quality control and verification of weather radar wind profiles.* J. Atmos. Oceanic Technol., **22**, 1541–1550.

Holleman, I, and H. Beekhuis (2005): *Evaluation of three Radar Product Processors*. Internal Report, KNMI IR-2005-03, 44 pp.

Holton, J.R. (1992): *An introduction to dynamic meteorology.* Academic Press, San Diego (CA), 511 pp.

Waldteufel, P. and H. Corbin (1979): *On the analysis of single Doppler data.* J.Appl. Meteorol., **18**, 532–542.